

HIGH T_g FRP & CEMENTITIOUS ADHESIVE **Potential benefits in fire for NSM FRP strengthened reinforced concrete beams**

Iolanda Del Prete^a, Antonio Bilotta^a, Luke Bisby^b, Emidio Nigro^a

^aUniversity of Naples Federico II, Department of Structures for Engineering and Architecture, Naples, Italy

^bUniversity of Edinburgh, Institute for Infrastructure & Environment, School of Engineering, Scotland UK

Abstract

Near surface mounted FRP strengthening is potentially less prone to damage due to fire exposure than externally bonded FRP reinforcement (EBR), provided that: (a) an FRP strengthening material with high glass transition and decomposition temperatures (T_g and T_d , respectively); and (b) a bonding agent with low thermal conductivity and good thermal stability, are used. This paper presents a project undertaken on a specific high T_g and cementitious adhesive bonded NSM FRP strengthening system. Dynamic Mechanical Analysis (DMA) and Thermogravimetric Analysis (TGA) performed on the novel high T_g commercial CFRP bar yielded a T_g value of 220°C (based on $\tan\delta$ peak) and T_d of about 360°C. Thermal conductivity tests were also performed on the cementitious grout. The results were used to better explain the failure modes of NSM FRP strengthened reinforced concrete beams at elevated temperature. The paper highlights the importance of understanding the thermo-mechanical properties of the various constituent materials for improving the performance of FRP strengthening systems in fire.

Keywords: NSM-FRP, DMA, TGA, fire testing

1 INTRODUCTION

The Near Surface Mounted (NSM) strengthening technique experienced widespread interest in recent years as an alternative to Externally Bonded Reinforcement (EBR). In the NSM technique the FRP bar/rod/strip is applied in a groove cut into the concrete cover and bonded in place by filling the groove with an epoxy or cementitious adhesive. Several studies have demonstrated that NSM with epoxy adhesive exhibits superior bond behaviour compared with EBR (El-Hacha & Rizkalla, 2004; Foret & Limam, 2008; Bilotta et al, 2011). NSM is also less prone to damage, since the FRP is embedded in a groove and inside adhesive. Despite this, the effectiveness of epoxy adhesive may be reduced at elevated temperatures; cementitious adhesives may offer superior performance to epoxies, whilst also protecting (mechanically and thermally) the FRP. Ambient temperature cure epoxy adhesives are characterized by relatively low glass transition temperatures (T_g), however higher T_g values can be achieved for pultruded FRP which is processed at elevated temperature. This paper summarizes the results of Dynamic Mechanical Analysis (DMA) and Thermogravimetric Analysis (TGA) on a novel commercially available CFRP bar, along with results of thermal conductivity tests on cementitious adhesive. The results are used to highlight failure modes of NSM FRP strengthened concrete beams at elevated temperature.

2 EXPERIMENTAL PROGRAM

Tests are aimed to define the material physical properties that influence the behaviour at high temperature of the strengthening system, such as the T_g and T_d of the CFRP bar and the thermal conductivity of the cementitious grout.

2.1 Dynamic Mechanical Analysis

Dynamic Mechanical Analysis (DMA) provides information about the mechanical properties of a specimen placed in sinusoidal oscillation, as a function of time (t) and temperature, by a small

sinusoidal oscillating force. The applied stress determines a corresponding strain, which is shifted with a phase shift (δ) due to the viscous behaviour of the polymeric material. The ratio between the stress and the strain amplitude defines the modulus of the complex modulus E^* , which is the stiffness of the material (ISO 6721-1, ASTM D4092). E^* is composed of the real part, the storage modulus E' , and the imaginary part, the loss modulus E'' . According to ISO 6721-1: the storage modulus E' represents the stiffness of a viscoelastic material and it is proportional to the energy stored during a loading cycle; the loss modulus E'' represents the viscous portion and it is proportional to the energy dissipated, for example as heat, during one loading cycle. The ratio between the loss and the storage modulus represents the loss factor $\tan\delta$. This means that a high $\tan\delta$ is indicative of a material characterized by a high non-elastic strain component, and vice versa.

In order to define the glass transition temperature of the CFRP bar, Dynamic Mechanic Analyses were carried out through the analyzer shown in Fig. 1, according to the suggestion of ISO 6721-1.

The experimental program was made of 6 tests: 3 tests in single cantilever (SC, Fig. 2) configuration and 3 tests in three-point bending (TPB, Fig. 3) configuration. In single cantilever arrangement the specimen is firmly clamped on one end and excited on the other end, whereas in in three-point bending arrangement the ends are freely supported and the load is applied to the midpoint. The tests were conducted in single frequency (1 Hz), with a temperature rate $2^\circ\text{C}/\text{min}$ and by setting a displacement amplitude equal to 0.05 mm.

The specimens tested in SC configuration were 15 mm long with a rectangular cross section (about 1.5 mm x 6.5 mm). The specimens tested in TPB configuration were 40 mm long with a square cross section (about 3 mm x 3 mm). The CFRP bar, which was a round wound bar, was chopped in pieces 15 mm and 40 mm long and then the central part of each piece was extracted. The outer surface, made essentially of resin, was peeled off and accurately made smooth and clean.

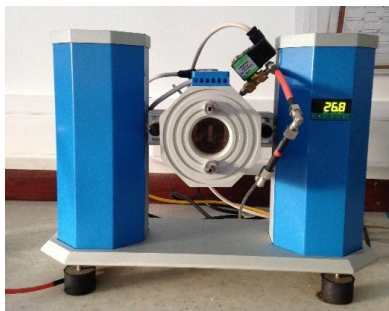


Fig. 1 Dynamic Mechanical Analyzer

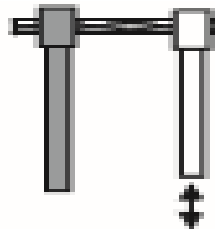


Fig. 2 SC configuration

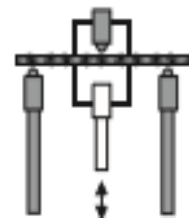


Fig. 3 TPB configuration

2.2 Thermogravimetric analysis

Thermogravimetric analysis (TGA) is an experimental technique, which provides the weight or the mass of a sample, measured as a function of temperature or time in isothermal experiments.

The TGA measurements are commonly depicted as a TGA curve, in which the mass is plotted versus temperature or time. In addition, a Differential Thermogravimetric (DTG) curve, which is the first derivative of TGA curve, provides the rate of mass changes versus temperature or time. The steps in TGA curve and peaks in DTG curve represent the mass loss, due to several effects, such as: loss of water of crystallisation; evaporation of volatile substances; chemical thermal decomposition in an inert atmosphere with generation of gaseous products; oxidative decomposition of organic substances in air or oxygen; other chemical reactions (Gabbott, 2008).

In order to define the decomposition temperature of the CFRP bar, Thermogravimetric Analyses were carried out through the Thermogravimetric Analyzer, shown in Fig. 4. This is a thermobalance with horizontal arrangement. The experimental program was made of 6 tests: 3 tests in Nitrogen (

N_2) atmosphere (50 $\mu\text{l}/\text{min}$) and 3 tests in air. The tested specimens were extracted by the core of the CFRP bar, through a procedure similar to that explained in section 2.1. The specimens with initial weight of about 50 mg were placed in the 70 μl alumina crucibles, which were set in the sample holder shown in Fig. 5. The tests were conducted with the temperature rate $10^\circ\text{C}/\text{min}$ in the temperature range $25\text{-}800^\circ\text{C}$.



Fig. 4 Thermogravimetric analyzer

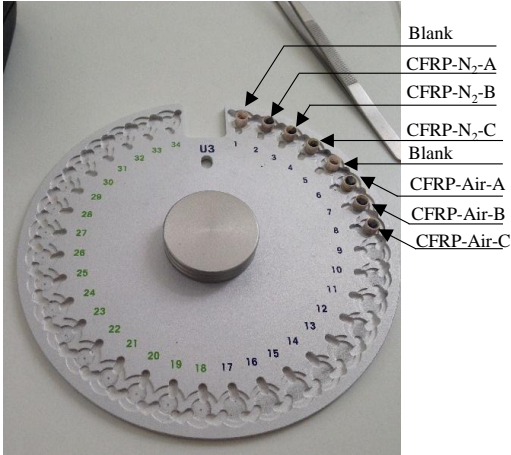


Fig. 5 Specimens placed in the aluminium crucibles (70 μl)

2.3 Thermal conductivity tests of cementitious grout

Tests were also performed to measure the thermal conductivity of the grout. It is a pumpable grout, high flow, unsanded, especially formulated for the grouting of CFRP bars in the typical groove of the NSM strengthening system. The water/cement ratio of the mix was set equal to 0.23, according to the manufacturer technical data sheet. Tests were conducted through the heat flow meter (see Fig. 6).

The heat flow meter measures the thermal conductivity of solid materials through a guarded heat flow meter. The specimen is placed between two plates controlled at different temperatures, resulting in a heat flow from the hotter (lower) to the colder (upper) plate (Fig. 7). A thin heat flux transducer, attached to the lower plate, measures the amount of heat. A cylindrical guard heater, maintained at or near the mean sample temperature, surrounds the sample, in order to minimize lateral heat transfer. Built-in thermocouples measure the overall temperature difference between the two surfaces in contact with the sample. The test sample is a cylinder, 50 mm of diameter and maximum 20 mm thick (Fig. 8). The tests were conducted at temperatures 50°C , 100°C , 150°C , 175°C .



Fig. 6 Heat flow meter

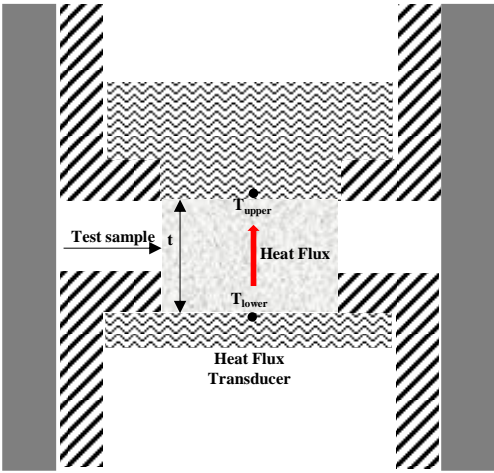


Fig. 7 Scheme of Heat flow meter

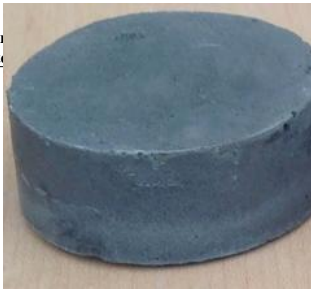


Fig. 8 Specimens of cementitious mortar

3 TESTS RESULTS AND DISCUSSION

3.1 Glass transition temperature

Various standards (ISO/CD 6721 - 11:2008; DIN 65 583, 1999) and apparatus manufacturers provide several proposals for determining the glass transition temperature in practice.

The most common techniques are: evaluation of the peak of the loss factor $\tan \delta$; 2% offset method; tangent method; inflection point method.

Fig. 9 plots the storage modulus E' , the loss modulus E'' and the loss factor $\tan \delta$ versus the temperature, referring, for example, to a test performed in TPB. This figure shows that $T_{g, \max \tan \delta}$ is about 215°C. Fig. 10 and Fig. 11 plot the storage modulus E' normalized to the storage modulus at temperature $T=70^\circ\text{C}$ ($E'_{70^\circ\text{C}}$) to define $T_{g, \text{offset}}$ and $T_{g, \text{onset}}$. The first is obtained in Fig. 10 through the intersection between the curve $E'-T$ and a line drawn parallel and 2% below the tangent to the linear portion of the curve $E'-T$. The second is obtained in Fig. 11 through the intersection between the tangents to the linear portion and to the inflection point of the curve $E'-T$. Finally, the temperature corresponding to the inflection point of the curve $E'-T$, $T_{g, \text{midpoint}}$, is calculated as the maximum of the first derivative of curve $E'-T$ plotted in Fig. 12.

Based on different definitions, the T_g of the bar ranges between 160°C ($T_{g, \text{offset}}$) and 220°C ($T_{g, \max \tan \delta}$). Note that the tests performed in TPB configuration yielded a T_g slightly higher (about 20°C) than that provided by the SC tests. It may be attributed to the softening of the resin in the clamped end in SC arrangement that led to a decrease of the constrain capacity. This resulted in a “un-real” faster decrease of the storage modulus compared to that provided by the TPB tests.

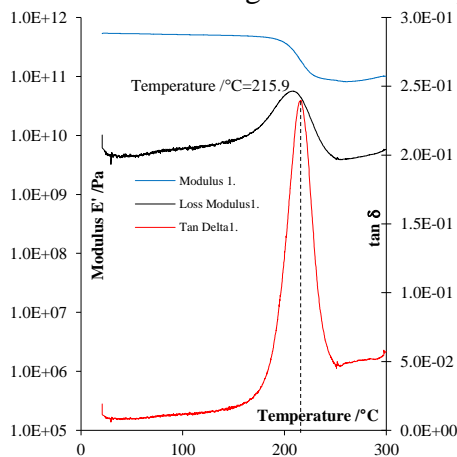


Fig. 9 E' , E'' and $\tan \delta$ vs temperature

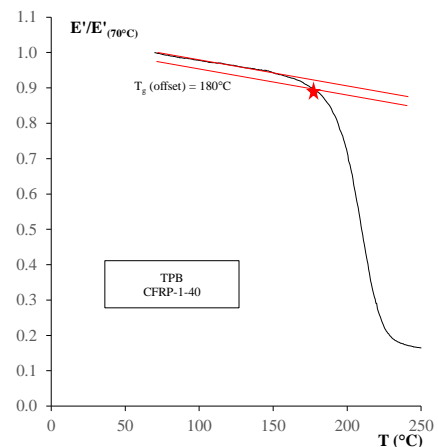


Fig. 10 Definition of T_g offset

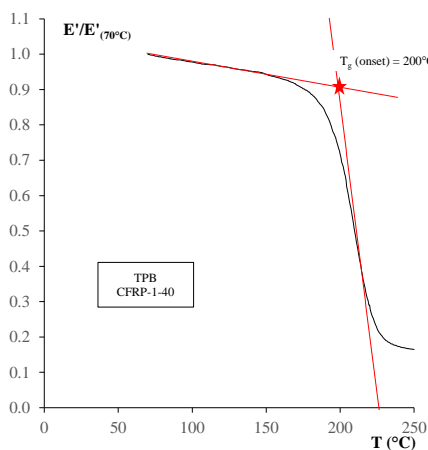


Fig. 11 Definition of T_g onset

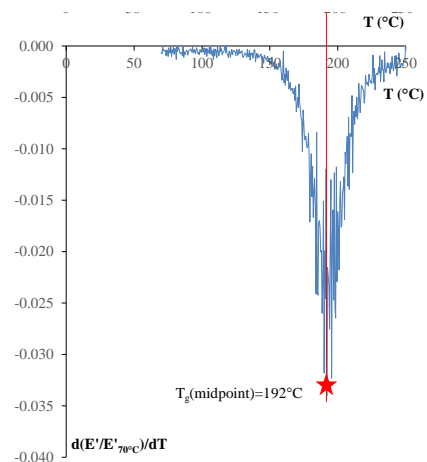


Fig. 12 Definition of T_g midpoint

3.2 Decomposition temperature definition

The results of the performed tests were represented in terms of weight loss versus temperature (TGA curves, Fig. 13) and First derivative of weight loss versus Temperature (DTG curves, Fig. 14). The material is very stable, since the scatter between the TGA curves, and similarly between the DTG curves, is very negligible. Moreover, when the decomposition occurred, the weight loss was about 27%. This means that the percentage in weight of fibres is about 73%.

As for the T_g , the decomposition temperature can be defined in various ways. The application of the above-mentioned methods on the TGA curves provided T_d values ranging between 320°C ($T_{d,offset}$) and 360°C ($T_{d,midpoint}$).

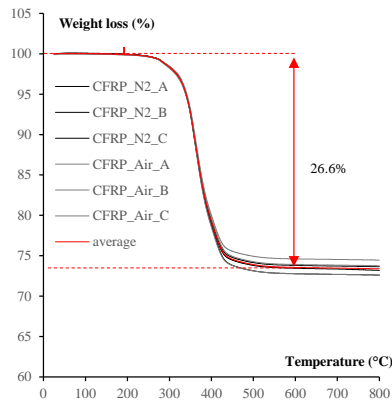


Fig. 13 TGA curves

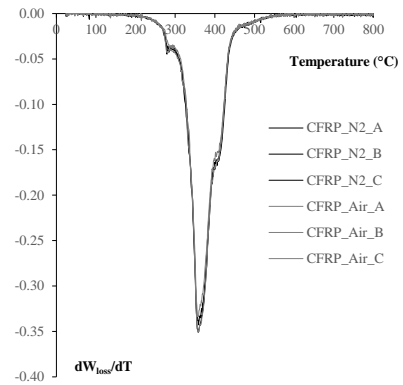


Fig. 14 DTG curves

3.3 Thermal conductivity of the cementitious mortar

The conducted tests showed that the thermal conductivity of the grout is almost constant in the temperature range 50-175°C and equal to about 0.55 W/(m K). Note that λ , only at 100°C, assumed a value equal to 0.66W/(m K). This is clearly related to the water evaporation at 100°C, which led to a greater energy absorption than that needed to maintain a certain gradient of temperature in the sample, at other testing temperatures. It can be concluded that this grout is a good insulator.

4 BENEFIT IN NSM FRP STRENGTHENING SYSTEM FOR RC BEAMS

Twelve flexural tests were performed on small-scale reinforced concrete beams 1450 mm long, 150 mm wide and 150 mm high strengthened in bending with a single NSM carbon FRP bar, and bonded using a cementitious grout rather than an epoxy adhesive. The tests were carried out at ambient (five tests) and elevated (seven tests) temperature on both un-strengthened and strengthened beams. Tests at high temperature were executed using propane-fired radiant panels. Two heating configurations were used, namely: (1) localised heating near midspan only; and (2) global heating over the entire bonded length of the FRP system. The thermo-structural response was investigated under loads typical of maximum permissible service strain conditions in the FRP. More details about the experimental program are shown in Del Prete et al, 2015.

The tests showed that the strengthening system is able to sustain loads typical of service conditions also at elevated temperature. The tests in global heating, conducted with a η_{fi} (ratio between the relevant effects of actions in the fire situation at time t , $E_{d,fi,t}$, and the design value of the resistance of the member in fire situation at beginning of thermally transient regime, $R_{d,fi,0}$) equal to about 0.7, showed that the attainment of $T_{d,midpoint}$ along the overall bonded length of the CFRP bar leads to the debonding of the strengthening system, due to slippage at bar/adhesive interface. The strengthening system of the beams tested with η_{fi} equal to about 0.7 in a local heating configuration, did not fail after 90 min of fire exposure, even when the temperature of the CFRP bar in the heated zone was equal to about 600°C. This means that the CFRP bar in the heated zone was completely debonded and the stress from the exposed zone was transferred to the effective cold

end-anchorage. Finally, the strengthening of the beams tested in a local heating configuration with η_{fi} equal to about 0.8 was not able to sustain the stress transferred from the midspan, when the maximum temperature in the CFRP bar near the midspan achieved about 600°C. It is very likely that the bar, close to the exposed zone, may have achieved the $T_{d,midpoint}$, due to the longitudinal thermal conductivity of the CFRP, leading to the reduction of the effective cold end anchorage length.

5 CONCLUSIONS

This paper presented a project undertaken on a specific high T_g and cementitious bonded NSM FRP strengthening system. Dynamic Mechanical Analysis (DMA) yielded a T_g ranging between 160°C ($T_{g,offset}$) and 220°C ($T_{g,max\tan\delta}$). Moreover, tests performed in different configurations (TPB and SC) yielded different values of T_g . Thermal Gravimetric Analysis (TGA), provided T_d values ranging between 320°C ($T_{d,offset}$) and 360°C ($T_{d,midpoint}$). All these variabilities in results, highlight the importance to standardize T_g and T_d definition as well as the test setup configuration.

Thermal conductivity tests confirmed the good insulation properties of the grout. Thermal conductivity is constant in the temperature range 50-175°C with a peak at 100°C, due to the water evaporation.

Moreover, the comparison of these results with flexural tests on the beam led to conclude that the loss of the bond between the CFRP bar and the cementitious grout probably occurs when $T_{d,midpoint}$ is attained.

ACKNOWLEDGMENTS

The authors would like to thank Milliken for providing the FRP materials and cementitious mortar (marketed under the trade name FireStrong) used in the experimental program.

REFERENCES

- ASTM D 4092 – 07 (2013). Standard Terminology for Plastics: Dynamic Mechanical Properties
- Bilotta A., Ceroni F., Di Ludovico M., Nigro E., Pecce M., 2011. *Bond Efficiency of EBR and NSM FRP Systems for Strengthening Concrete Members*, J. Compos. Constr. 2011.15:757-772
- Burke P.J., Bisby L. A., Green M., 2013. Effects of elevated temperature on near surface mounted and externally bonded FRP strengthening systems for concrete, *Cement & Concrete Composites* 35 (2013) 190–199
- Del Prete I., Bilotta A., Bisby L., Nigro E., 2015. *Flexural tests on RC beams strengthened with NSM FRP bars bonded with cementitious grout*, FRPRCS-12 & APFIS-2015 Joint Conference, 14-16 December 2015, Nanjing, China
- DIN 65 583 (1999). Aerospace - Fibre reinforced concrete materials - Determination of glass transition of fibre composites under dynamic load
- El-Gamal S., Al-Salloum Y., Alsayed S., Aqel M., 2012. *Performance of near surface mounted glass fiber reinforced polymer bars in concrete*. *Journal of Reinforced Plastics and Composites*, 31 (22) 1501–1515 DOI: 10.1177/073168441246408
- El-Hacha R., Rizkalla S: H., 2004. Near-Surface-Mounted Fiber-Reinforced Polymer Reinforcements for Flexural Strengthening of Concrete Structures, *ACI Structural Journal*, September-October 2004, 717-726
- Foret G., Limam O., 2008. Experimental and Numerical analysis of RC two-way slabs strengthened with NSM CFRP rods, *Construction and Building Materials* 22 (2008) 2025-2030
- Gabbott P. (2008). *Principles and Applications of Thermal Analysis*, Blackwell Publishing
- ISO 6721-1:2011. *Plastics - Determination of dynamic mechanical properties - Part 1: General principles*
- Palmieri A., Matthys S., Taerwe L., 2013. Fire Endurance and Residual Strength of Insulated Concrete Beams Strengthened with Near-Surface Mounted Reinforcement, *J. Compos. Constr.* 2013.17:454-462
- Petri P., Blaszak G., Rizkalla S., 2013. *Structural Fire Endurance of an RC Slab Strengthened with High T_g Near Surface Mounted CFRP Bars*. Conference Proceedings ACIC 2013, Edited by Miss Claire. J. Whysall and Prof. Su. E. Taylor, 140-151, Queen's University Belfast on 10 -12 September 2013